

Novel cellular evidence of lipophagy within the Sertoli cells during spermatogenesis in the turtle

Nisar Ahmed^{1,2}, Yi Liu¹, Hong Chen¹, Ping Yang¹, Yasir Waqas¹, Tengfei Liu¹, Jameel Ahmed Gandahi³, Yufei Huang¹, Lingling Wang¹, Xuejing Song¹, Imran Rashid Rajput², Taozhi Wang¹, Qiusheng Chen¹

¹Laboratory of Animal Cell Biology and Embryology, College of Veterinary Medicine, Nanjing Agricultural University, Nanjing, Jiangsu Province 210095, China

²Faculty of Veterinary and Animal Sciences, LUAWMS, Uthal 90150, Pakistan

³ Faculty of Animal Husbandry and Veterinary Sciences, Sindh Agriculture University, Tando Jam 70060, Pakistan

Correspondence to: Qiusheng Chen; email: chenqsh305@njau.edu.cn

Keywords: spermatogenesis, lipophagy, Sertoli cell; LC3, Chinese soft-shelled turtle

Received: July 31, 2016 Accepted: September 30, 2016 Published: October 16, 2016

ABSTRACT

Spermatogenesis is a complex process producing haploid spermatozoa, and the formation of lipid droplets (LDs) within Sertoli cells is critical to maintaining normal spermatogenesis. However, the utilization of LDs within Sertoli cells is still largely unknown. In the present study, proliferation of spermatogonial cells had begun in May, whereas the meiotic cells occurred predominately in July and majority of spermiogenic cells were observed in the seminiferous tubules in October. However, TEM and Oil Red O staining demonstrated that a larger number of LDs had accumulated within the Sertoli cells in May compared to that in October. There were several LDs attached to the isolation membrane/phagophore, suggesting that the LDs may be a source of endogenous energy for the biogenesis of autophagosomes. The LDs were enclosed within the autophagosomes in May, whereas, autophagosomes and mitochondria were directly attached with large LDs within the Sertoli cells in October. Furthermore, immunohistochemistry results demonstrated the stronger localization of LC3 on the Sertoli cells in May than in October. This study is the first to provide clear evidence of the two different modes of lipophagy for lipid consumption within Sertoli cells, which is a key aspect of Sertoli germ cell communication during spermatogenesis.

INTRODUCTION

Spermatogenesis is a complex process of male gamete production with successive cellular differentiation that occurs with the support of the Sertoli cells. This process consists of the proliferation of progenitor cells (spermatogonial mitosis), which undergo reduction divisions, segregation and recombination of genetic material, known as spermatocytic meiosis, and maturational or spermiogenic phases, which are the final aspect of spermatogenesis [1, 2]. Once the population of germ cells has reached maturation, spermiation consequently occurs, and the germ cells are released as spermatozoa from the seminiferous epit-

helium within the testes of vertebrates [3-5]. Few studies have described the major steps of spermatogenesis (light and electron microscopy) in more than several species of reptilian taxon, such as the Ophidia (snakes), the temperate lizard (*Podarcis muralis*) and the turtle (*Trachemys scripta*), but even in these studies, the ultrastructure is mainly focused on spermiogenesis and the mature spermatozoon. The ultrastructure of the early stages of spermatogenesis has not been well explored in Reptilia [3, 6, 7], and the ultrastructure of spermatogenesis within the Chinese soft-shelled turtle, *Pelodiscus sinensis*, has not yet been reported, although its spermiogenesis has been observed [8].

Germ cells advance through development in association with Sertoli cells, which play a central role in the control of spermatogenesis. The key functions of Sertoli cells as reported in mammals, are providing structural support, phagocytosing degenerating germ cells, protecting the germ cells, releasing spermatids at spermiogenesis and nourishing the developing germ cells [9, 10]. Sertoli cells are also involved in the formation of LDs, the cytoplasmic stores of neutral lipids, but the existence of these lipid inclusions within Sertoli cells exhibits variation throughout spermatogenesis in rat testes [11]. The utilization of lipids is critical to maintain cellular energy homeostasis for different cellular processes. During nutrient scarcity, cellular lipids stored as triglycerides in LDs are hydrolyzed into fatty acids for energy. Previous studies have found that the formation of LDs is associated with the process of the phagocytosis of residual bodies or apoptotic cells within Sertoli cells, which was detected by Oil Red O staining [12]. Recently, autophagy has also been implicated in neutral lipid utilization from droplets under starvation conditions in mouse hepatocytes [13].

Autophagy is an intracellular degradation system conserved among eukaryotes, and a prominent feature of autophagy is the dynamic membrane reorganization that results in the formation of double-membrane spherical structures known as autophagosomes. The contents of the autophagosome are then degraded by lysosomes, which are primarily needed to supply nutrients. [14]. When this double membrane structure develops around the lipid droplets, it is termed the lipophagosome, and the process is called lipophagy [15, 16]. Autophagy is regularly monitored with the LC3, a specific marker to detect autophagosome by light microscopy. LC3, microtubule-associated protein light chain 3, is a mammalian homolog of yeast Atg8, when autophagosome biogenesis starts, LC3 is conjugated with phosphatidylethanolamine and localizes on the inner and outer autophagic membranes or autophagosomes [17]. Recently, it has become evident that autophagy plays an active role in Sertoli cells [18-21]; it is involved in the clearance of androgen binding protein (ABP) in rat Sertoli cells and in the assembly of ectoplasmic specialization within mouse Sertoli cells [19, 22]. However, the role of autophagy in Sertoli cells is still largely unknown [22].

The objectives of the current study were to establish a detailed analysis of germ cell development strategy and ultrastructure and to explore the *in vivo* role of lipophagy in the consumption of LDs within Sertoli cells in the testes of the Chinese soft-shelled turtle, *Pelodiscus sinensis*.

RESULTS

Light microscopy

The testis of the Chinese soft-shelled turtle consisted of seminiferous tubules lined with developing germ cells and a permanent number of Sertoli cells. In May, the seminiferous epithelium contained numerous mitotic cells (proliferative spermatogonia) and a few early spermatocytes, which indicated an early stage of spermatogenesis (Figs. 1A, 1B). By July, pachytene spermatocytes were detected in the seminiferous epithelium. The majority of the germ cell population was meiotic cells (spermatocytes) with some round/elongated spermatids progressing through the early events of spermiogenesis. These differentiating spermatids were arranged in the sperm column within the pockets of the Sertoli cells, but the lumen of the seminiferous tubule remained clear (Figs. 1C, 1D). In October, the seminiferous epithelium was lined with numerous spermatids that were progressing into various phases of spermiogenesis, and the lumen was filled with free spermatozoa. The meiotic activity of the germinative epithelium was largely completed in the seminiferous tubules, and the meiotic cells were drastically reduced at this stage. Few resting spermatogonia and Sertoli cells were observed around the basal membrane (Figs. 1E, 1F).

Immunohistochemistry (IHC)

The immunohistochemistry for LC3, which is a specific marker for autophagosomes, was observed in the testis of the Chinese soft-shelled turtle. Immunohistochemistry demonstrated strong immunoreactivity in the Sertoli cells in May (Fig. 2A), and weak immunoreactivity was noted in October (Fig. 2B).

Oil red O (ORO) staining

The ORO staining was performed in the testis for LD analysis in the Sertoli cells during spermatogenesis. The results indicate that a large number of LDs accumulated within the Sertoli cells in May. In contrast, few LDs were observed within the Sertoli cells in October, and more localization was observed around the elongated spermatids at this time (Fig. 3A, 3B).

Transmission electron microscopy (TEM)

In May, three different types of spermatogonia were observed in the seminiferous epithelium, such as stem cells, type-A spermatogonia and type-B spermatogonia. The large population of these spermatogonia cells was accumulated near the basement membrane in the seminiferous epithelium. The stem cells appeared to be

the smallest of the spermatogonia with their nuclei ovoid in shape without a nucleolus. The type-A spermatogonia were observed as ovoid in shape along with nuclei, which contained very little heterochromatin and had one flattened cellular surface resting directly on the basement membrane. The type-B spermatogonia contained round nuclei, including a prominent nucleolus and several large globules of heterochromatin within the nucleoplasm (Figs. 4A, 4B, 4C). A few early spermatocytes were also observed in the May samples, along with a large number of LDs. These LDs originated from the Sertoli cells during this phase of spermatogenesis (Figs. 4D, 4E, 5A). Several large LDs were detected around the isolation membranes/phagophore within the Sertoli cells during the development of autophagosomes (Figs. 5A, 5B). Then, the autophagosomes enclosed several LDs and mitochondria (Figs. 5C, 5D).

Type-B spermatogonia undergo mitotic divisions to produce primary spermatocytes (pre-leptotene), which are characterized by increasing nuclear and cytoplasmic size and the gradual condensation of nuclear chromatin into distinct chromosomes. Pre-leptotene spermatocytes contained a round nucleus and numerous mitochondria accumulated in one place (Fig. 6A). In contrast, leptotene spermatocytes appeared slightly larger than the pre-leptotene spermatocytes, and their nuclei contain fine filamentous chromatin fibers (Fig. 6B). The zygotene spermatocytes were noted by an increase in the thickening of the filamentous chromatin fibers within the nucleus and the synaptonemal complexes that started to appear (Fig. 6C). Pachytene spermatocytes contained well-developed synaptonemal complexes, which connected the homologous chromosomes during the first meiotic divisions. Thicker and dense chromo-

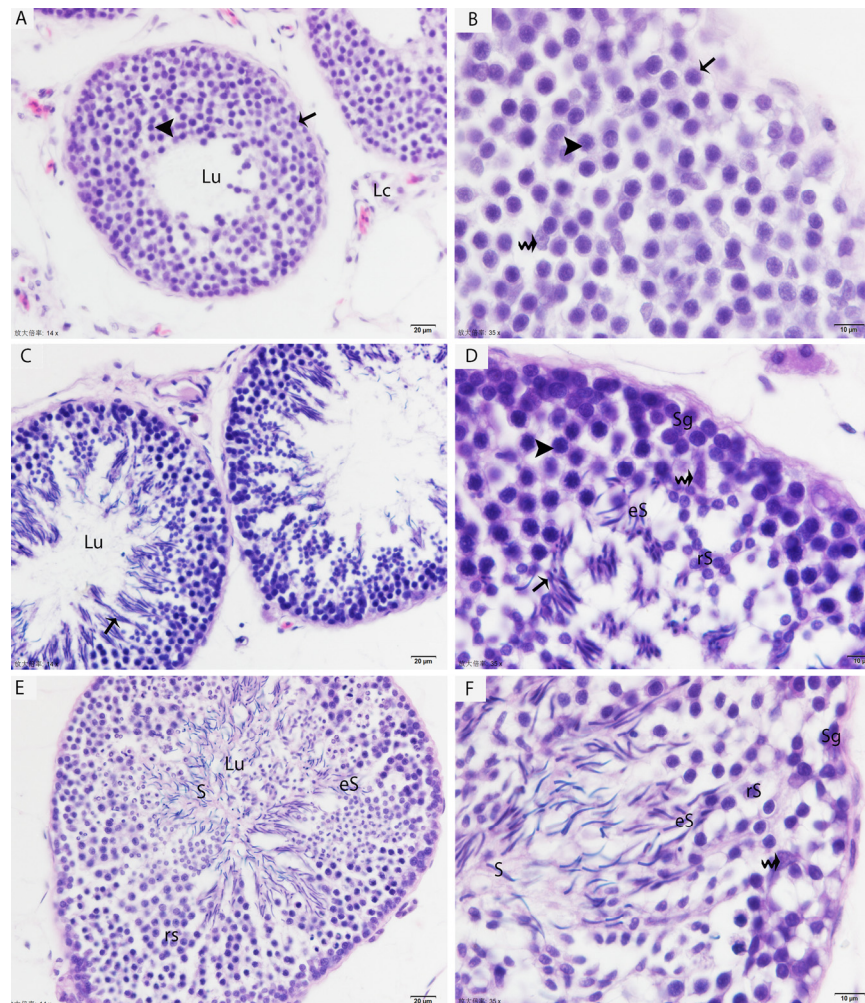


Figure. 1 Light micrograph shows the histological structure of testis. (A, B) Seminiferous tubules show the spermatogonia (arrow) and few leptotene spermatocytes (arrowhead) in May. (C, D) Pachytene spermatocytes (arrowhead), round/elongated spermatids are present in the seminiferous epithelium, and spermatids are arranged in the sperm column (arrow) in July. (E, F) The round/elongated spermatids as well as free spermatozoa in the lumen and few spermatogonia are observed in October. LC: Leydig cell; Sg: spermatogonia; rS: round spermatid; eS: elongated spermatid; S: spermatozoa; Lu: lumen; (curved arrow): Sertoli cells. H & E stain. Scale bar= 20 μ m (A, C, E) and 10 μ m (B, D, F).

somes were attached with spindle fibers along with the centriole and the Golgi complexes that were found close to the centrosome (Figs. 6D, 6E, 6F, 6G). The diplotene spermatocytes appeared with thick fully condensed chromosomal fibers that were interspersed with large open areas of nucleoplasm (Fig. 6H). Meiosis I progressed to produce secondary spermatocytes, which appeared with nuclei along with nucleolus. There were few nuages that developed, and vacuolated mitochondria were observed in the secondary spermatocytes (Fig. 6I).

In October, the majority of germ cell types within the seminiferous epithelium were spermiogenic cells (round or elongated spermatids), which were characterized by the development of the acrosomic system, the elongation of the nucleus, and the condensation of chromatin material, as suggested by Russell [4]. The

spermatids appeared with spherical nuclei, which were centrally located and contained chromatin bodies (Fig. 7A). The 7 steps of spermatids were observed during spermiogenesis; the first four steps of round spermatids (S1, S2, S3, and S4) represent the acrosome phase of development. The acrosomal vesicle was in direct contact with the nuclear envelope and pressed against the nuclear wall, in which it formed a wide shallow depression. This depression progressively increased in the nucleus from Step1 to Step2, Step3 and Step4 spermatids. Meanwhile, the elongation and condensation of chromatin within the nucleus characterized Step5, Step6 and Step7 spermatids. These spermatids existed in the bundles within the pockets of the Sertoli cells, consequently forming the sperm column (Figs. 7A, 7B). During the spermiogenic phase, the processes of the Sertoli cells contained several lipid droplets, autophagosomes and abundant mitochondria.

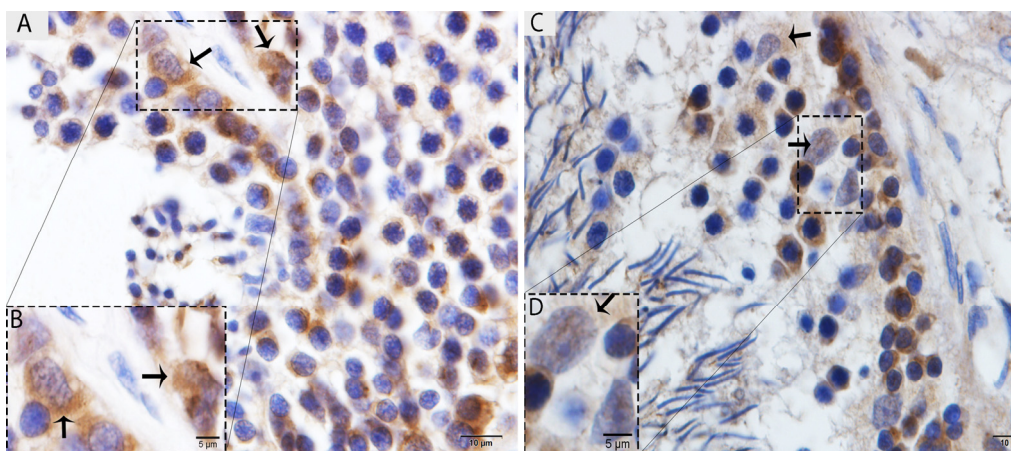


Figure 2. Light micrograph of LC3 localization in the testis. (A) The immunoreactivity shows strong positive expression on the Sertoli cells in May. (B) A higher magnification of the rectangular area. (C) Weak, positive expression on the Sertoli cells in October. (D) Illustration of rectangular area. Scale bar= 10 μ m (A, C) and 5 μ m (B, D).

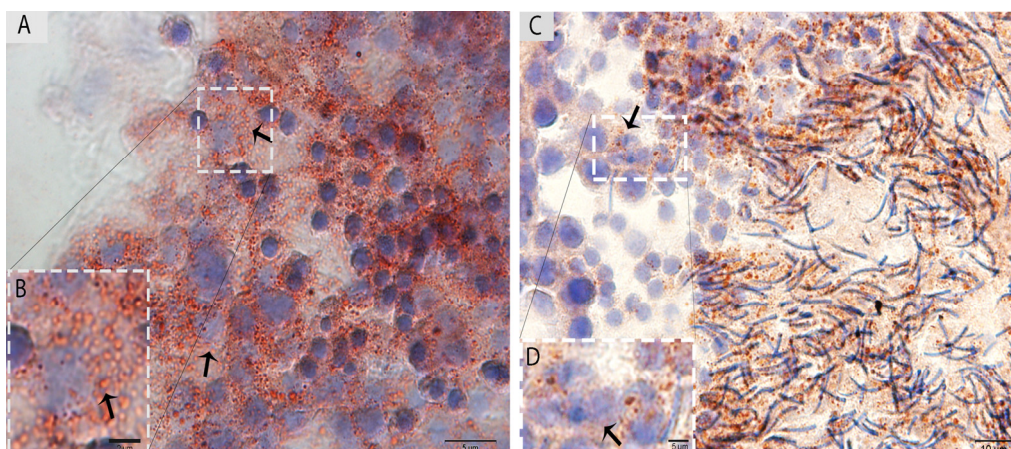


Figure 3. Light micrograph of Oil Red O staining in the testis. (A) The ORO staining shows a large number of lipid droplets in the Sertoli cells (arrow) in May. (B) A higher magnification of the rectangular area. (C) Lower numbers of lipid droplets in the Sertoli cells (arrow) in October are observed. (D) Illustration of the rectangular area. Scale bar= 10 μ m (A, C), 2 μ m (B) and 5 μ m (D).

These autophagosomes and mitochondria were attached to the large LDs (Figs. 8A, 8B). Detailed descriptions

about spermiogenesis have been described in an earlier study by our research group [8].

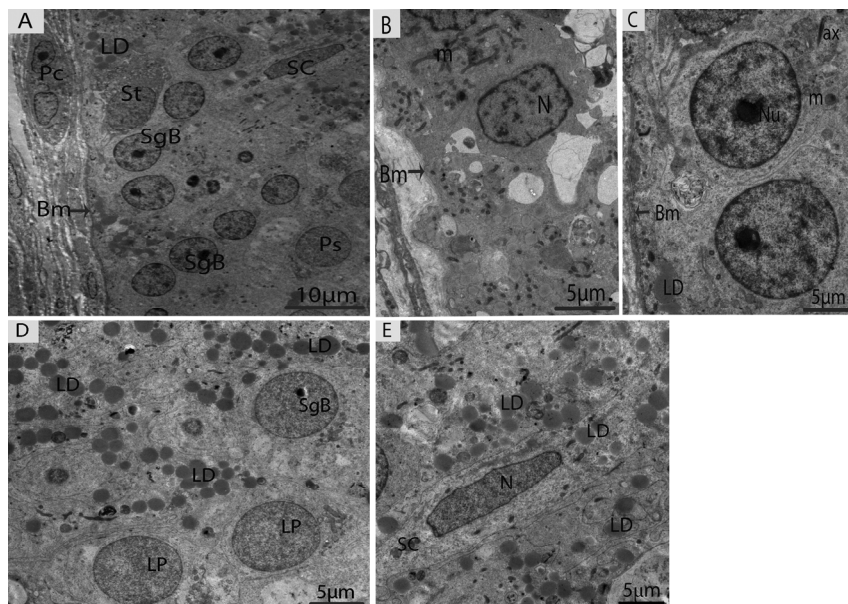


Figure 4. Electron micrograph of seminiferous tubules in May. (A) Seminiferous tubules contain type B spermatogonia and early spermatocytes. (B) Type-A spermatogonia. (C) Type-B spermatogonia. (D) The numerous lipid droplets are observed around leptotene spermatocytes. (E) Sertoli cells contained lipid droplets. Bm: basal membrane; SgB: spermatogonia type B; Ps: primary spermatocyte; SC: Sertoli cell; LD: lipid droplets; Lp: leptotene spermatocyte; N: nucleus; m: mitochondria; ax: axonome; Pc: peritubular cell; St: stem cell. Scale bar= 10µm (A) and 5µm (B, C, D, E).

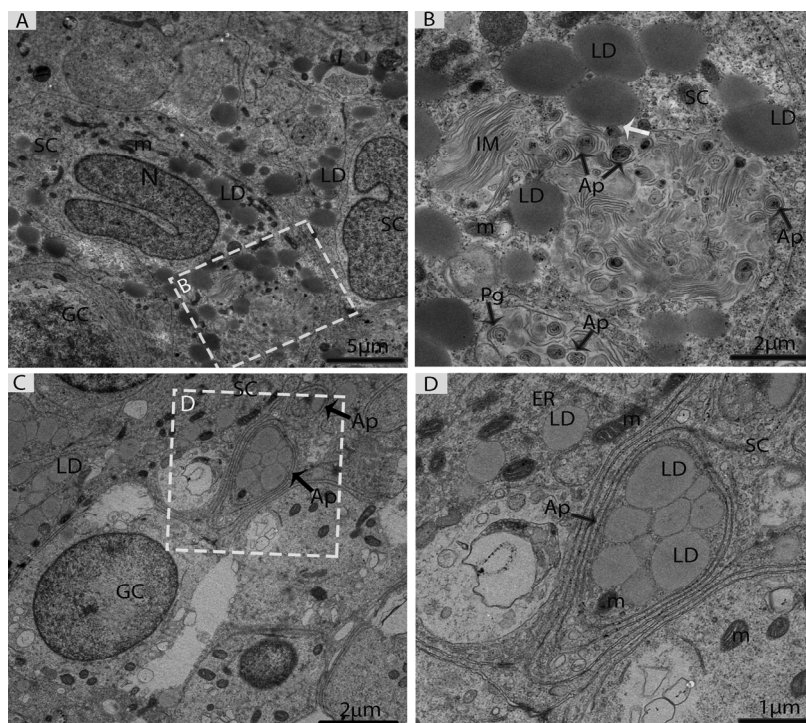


Figure 5. Electron micrograph of Sertoli cells during consumption of lipid droplets via lipophagy in May. (A) Sertoli cells contained numerous lipid droplets. (B) Illustration of Fig. A (rectangular area) shows the lipid droplets in contact with a phagophore and autophagosomes (white arrow). (C) Lipid droplets enclosed in the autophagosome. (D) Higher magnification of the square from Fig. C. SC: Sertoli cell; LD: lipid droplets; IM: isolation membranes; Ap: autophagosome; Pg: phagophore; GC: germ cell; m: mitochondria; ER: endoplasmic reticulum. Scale bar= 5µm (A), 2µm (B, C) and 1µm (D).

DISCUSSION

Spermatogenesis within the seminiferous epithelium of the Chinese soft-shelled turtle, *Pelodiscus sinensis*, was closely parallel to that previously reported in the slider turtle [23]. In the present study, the proliferation of germ cells started in May; meiotic cell division peaked in July, and spermiogenesis largely was complete in October. Consequently, spermiation occurred in November with a remaining period of spermatogenic quiescence (December to April) [24]. The sperm development in the *Pelodiscus sinensis* seemed to be a postnuptial pattern, which is consistent with the pattern observed in *A. ferox* and *Trachemys scripta* [25]. In contrast, although spermatogenesis within most lizards follows a prenuptial pattern of development, it is followed by a comparatively shorter quiescence period [26]. Germ cell development starts in midsummer, continues throughout winter and is completed by the

following June in the lizards [6, 27]. This divergence in timing probably resulted from different environmental conditions related with temperature in the respective regions of the animals studied.

The majority of the soft-shelled turtle's germ cell population progressed through the phases of spermatogenesis (proliferation, meiosis, and spermiogenesis) as a single cohort within the seminiferous epithelium. Furthermore, the germ cell development strategy of this turtle was found to be temporal in nature, which is consistent with that found in other temperate-zone reptiles, (wall lizard, black swamp snake, slider turtle, and alligator) [6, 7, 23]. In contrast, all other amniotic germ cell development strategies (birds and mammals) result in waves of sperm being released throughout the active months of the testes [4, 28, 29]. In the current study, five to six generations of spermatids within the seminiferous epit-

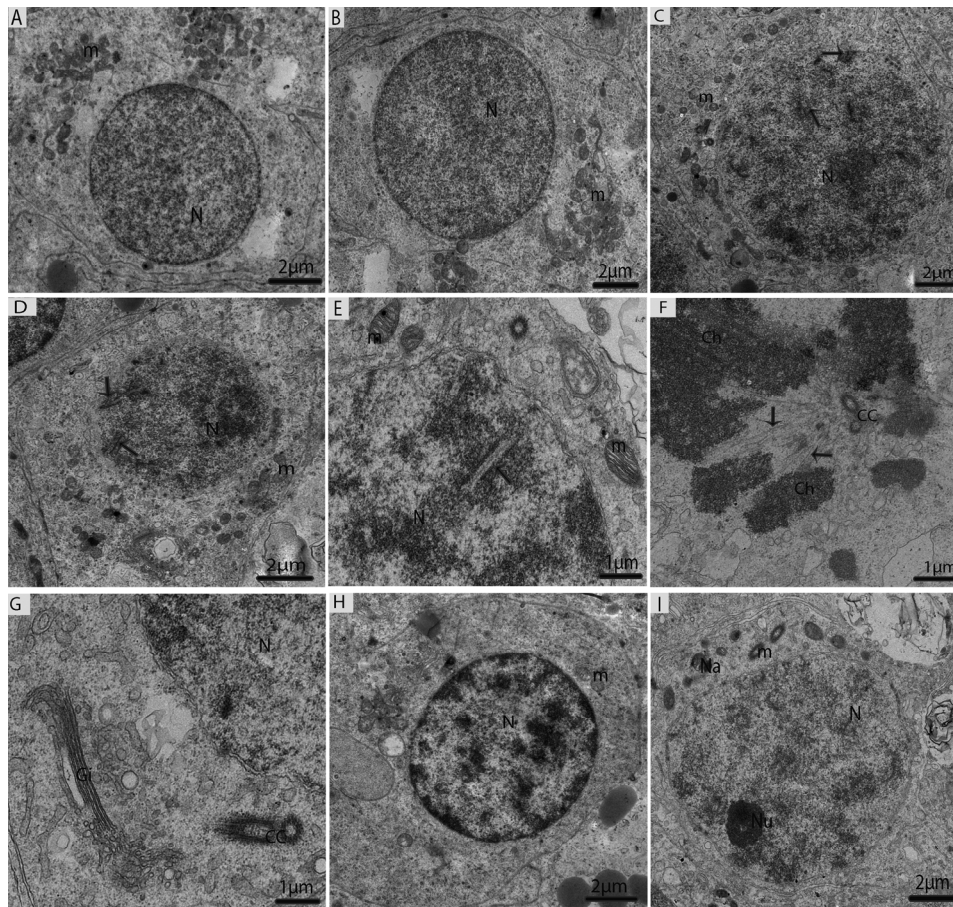


Figure 6. Electron micrograph of meiotic cells in July. (A) Primary spermatocytes in pre-leptotene stage. (B) Primary spermatocytes in leptotene. (C) Primary spermatocyte in zygotene beginning to form synaptonemal complexes (arrow). (D) Primary spermatocyte with visible synaptonemal complexes (arrow) in pachytene. (E) Synaptonemal complexes (arrow). (F) Thicker and dense chromosomes are attached with spindle fibers (arrow). (G) Golgi complex is observed close to the centrosome. (H) Primary spermatocytes in diplotene. (I) Secondary spermatocytes containing vacuolated mitochondria, including a few nuages. N: nucleus; m: mitochondria; Ch; chromosomes; CC: centrosome; Na: nuage; Gi: Golgi apparatus. Scale bar= 2µm (A, B, C, D, H, I) and 1µm (E, F, G).

helium were observed at the same time in October, which is much different than that found in birds and mammals [4]. These elongating steps of spermiogenesis were apically accumulated within the pockets of the Sertoli cell processes and were released in the lumen with spermiation [24]. Moreover, we observed numerous LDs within the Sertoli cells in May than in October by TEM and ORO staining, and our previous study reported that the Sertoli cells contain abundant LDs during early spermatogenesis as compared to late spermatogenesis [30]. These LDs can be used for nourishing the germ cells. However, it was found that the Sertoli cell lipids were absorbed into spermatids during the different stages of spermatogenesis and that lipid inclusions can be transferred from the Sertoli cells to primary spermatocytes [12, 16, 31]. Many reptilian Sertoli cells undergo a well-defined lipid cycle that

corresponds to spermatogenic activity, but the metabolism of lipids in the Sertoli cells remains an open question [12, 32, 33].

We found, for the first time, the close contact of numerous LDs with the isolation membranes/the phagophore during the formation of autophagosomes within Sertoli cells (Fig. 4B). When two organelles come into contact in kiss-and-run events, it may allow a direct exchange of the material [34]. Hence, we suggested that the LDs regulate autophagosome biogenesis by donating lipids to the outside membrane of the phagophore, as suggested by Dupon and his coworkers [34]. The mechanism of autophagosome biogenesis is a remarkable cell biology problem because it stands apart from the canonical vesicular trafficking process [35-37]. Shpilka et al. [37] further reported that

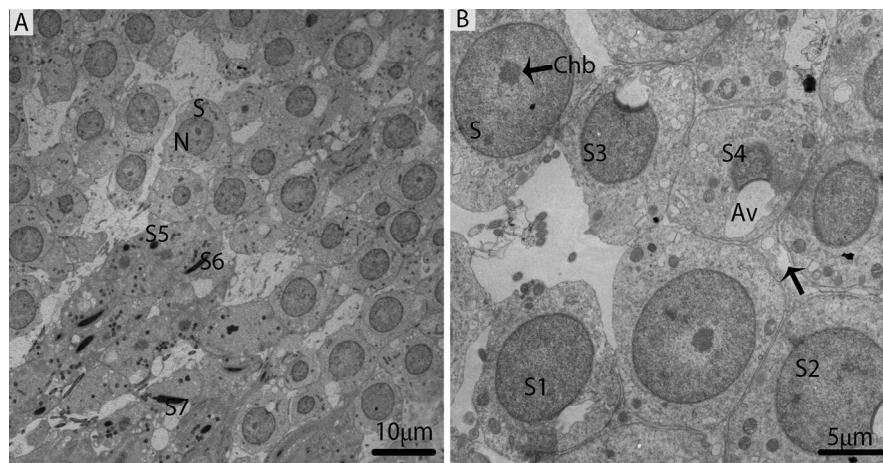


Figure 7. Electron micrograph of seminiferous tubules in October. (A) The majority of cell types within the seminiferous tubules are round/elongated spermatids. (B) Different stages of spermiogenic cells. S: spermatid; eS: elongated spermatid; SC: Sertoli cell; Sp: spermatid; Av: acrosomal vesicle; Chb: chromatin body; (arrow). Scale bar= 10µm (A) and 5µm (B).

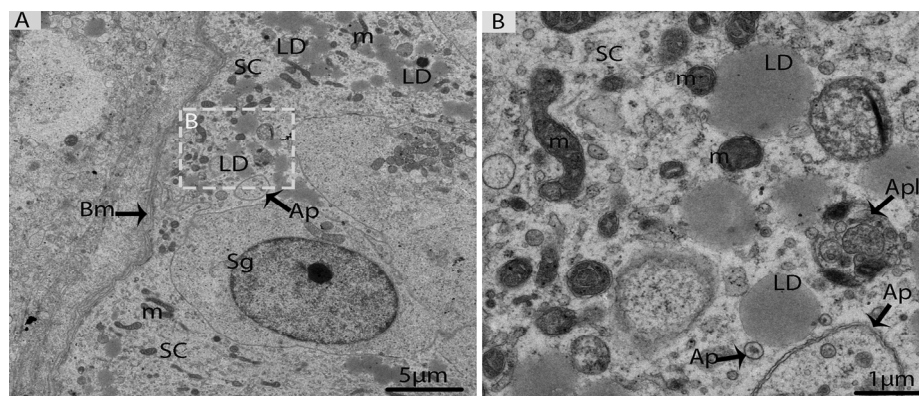


Figure 8. Electron micrograph of Sertoli cells in October. (A) Sertoli cells appeared with lipid droplets mitochondria and autophagosomes. (B) Illustration of panel A (rectangular area) clearly shows the mitochondria and autophagosomes attached to lipid droplets. SC: Sertoli cell; Sg: spermatogonia; Bm: basal membrane; Ap: autophagosome; Apl: autophagolysosome; LD: Lipid droplets; m: mitochondria. Scale bar= 5µm (A) and 1µm (B).

the order in the relationship between autophagy and LDs, instead of being a substrate for lipophagy, is that the LDs act as contributors for autophagosome biogenesis in kiss-and-run events.

Another widely accepted relationship is that autophagosomes can engulf LDs in a process known as “lipophagy” [16], which includes lysosomal lipolysis and the release of fatty acids for metabolic needs [38, 39]. Current findings provided clear evidence that several LDs were enclosed within the double membrane autophagosomes in the Sertoli cells in May (early spermatogenesis) (Fig. 4C). In other words, autophagosomes and mitochondria were directly attached to the LDs in October, which suggests that lipophagy is involved in lipid metabolism to release endogenous energy for the developing germ cells in two different ways because lipid droplets always provide energy to different cells [16, 40]. Furthermore, our immunohistochemistry findings demonstrate the stronger positive expression of LC3 in the Sertoli cells in May than in October, which indicates that autophagy is persistent throughout the process of spermatogenesis, but the number of autophagosomes within Sertoli cells is reduced in late spermatogenesis (October). Moreover, Akiko et al. [41] suggested that electron microscopy, along with LC3 localization, can confirm the presence of autophagosomes. Hence, our LC3 localization and TEM findings are inline regarding the existence of autophagosomes within the Sertoli cells.

In conclusion, the mode of spermatogenesis in the Chinese soft-shelled turtle, *Pelodiscus sinensis*, is temporal in nature and is also commonly found in other temperate-breeding reptiles. Moreover, this study provides novel morphological evidence on the involvement of autophagy in the mobilization of LDs within Sertoli cells in two different ways. Several LDs were found during autophagosome biogenesis in the Sertoli cells. The autophagosome enveloped several LDs in May (early spermatogenesis), while it was directly attached to LDs in October (late spermatogenesis), implying that this process becomes a source of endogenous energy for the different spermatogenic events. This research describes a new role of lipid metabolism through lipophagy within Sertoli cells during the process of spermatogenesis, and understanding this particular set of relationships may be highly valuable.

MATERIALS AND METHODS

Animals

15 mature male (3-4 years-old) Chinese soft-shelled turtles *Pelodiscus sinensis* were captured from an aqua farm in Nanjing, Jiangsu province of China in May,

July and October, five turtles during each time period. The animals were rendered comatose using intraperitoneally administered sodium pentobarbital (20 mg/animal) and were sacrificed by cervical dislocation. The testes were collected immediately and fixed to performed different techniques (details below). Sample preparation was conducted according to accepted international standards and was approved by the Ethics Committee for Animal Care and Use by the Science and Technology Agency of Jiangsu Province (SYXK (SU) 2010-0009).

Light microscopy

The testis samples were placed in 10% neutral buffered formalin for fixation overnight, and then embedded in paraffin wax. Sectioning was done at 5 μ m. These sections were stained with hematoxyline and eosin procedures (Harry’s hematoxyline for 2 min and 1% eosin for 30 sec) for light microscopic analysis using an Olympus microscope (BX53), camera (Olympus DP73), Japan.

Immunohistochemistry (IHC)

The immunohistochemical staining for LC3 was performed according to the manufacturer’s recommendations and as suggested in previous studies [42, 43]. Testis specimen sections were processed using a standard immunohistochemistry protocol, as previously described [44]. Briefly, after deparaffinization, blocking endogenous peroxidase, microwave antigen retrieval, and BSA (Bull Serum Albumin) blocking, the primary antibody of rabbit polyclonal anti-LC3B (ab48394, Abcam, Cambridge, UK) was applied for 1 h at room temperature. After washing with PBS, the slides were incubated for 30 min with goat anti-rabbit-biotinylated antibody. The peroxidase was visualized with DAB, and sections were counter stained with hematoxyline. Sections incubated in PBS alone served as negative controls.

Oil Red O (ORO) staining

For ORO staining, samples of the testis (May and Oct.) were washed 255 with PBS, fixed with 4% formaldehyde for 10 min, and stained with ORO (Sigma) 256 solution (oil O-saturated solution in isopropanol: water, 3:2) for 15 min as previous 257 description. Then, the sections were washed with 70% alcohol for 5s to remove 258 background staining.

Transmission electron microscopy (TEM)

The specimen of testis were cut into small parts (1 mm³), and fixed into 2.5% glutaraldehyde in PBS (4°C,

pH 7.4, 0.1 M) for 24h. Specimen were rinsed in the same PBS and then post-fixed for 1h. at room temperature in the same way by using buffered 1% osmium tetroxide (Polysciences Inc. Warrington, PA, USA) and then washed in the buffer. The samples were dehydrated in ascending concentrations of ethyl alcohol, infiltrated with a propylene oxide–Araldite mixture and then embedded in Araldite. The blocks were then sectioned by using an ultramicrotome (Reichert Jung, Wien, Austria) and the ultrathin sections (50 nm) were mounted on copper coated grids. The specimens were stained with 1% uranyl acetate and Reynold’s lead citrate for 20 min. Finally specimen were examined and photographed by using a high resolution digital camera (16 mega pixel) connected to the TEM (Hitachi H-7650, Japan).

CONFLICTS OF INTEREST

The authors have no conflict of interest to declare by authors.

FUNDING

This work was supported by the National Natural Science Foundation of China (grant number 31272521 and 31672505) and Priority Academic Program Development of Jiangsu Higher Education Institutions, PAPP.

REFERENCES

1. Hess RA, de Franca LR. Spermatogenesis and cycle of the seminiferous epithelium. *Molecular Mechanisms in Spermatogenesis*: (Cheng CY, ed.), 2009; pp. 1-15. Springer, New York.
2. Courot M, Hochereau-de Rivers MT, Ortavant R. Spermatogenesis. *The Testis*: (Johnson AD, Gomes WR, Van Demark NL, eds.), 1970; pp.339-432, NY: Academic Press, New York.
3. Gribbins KM, Rheubert JL. The ophidian testis, spermatogenesis and mature spermatozoa. *Reproductive Biology and Phylogeny of Snakes*. (In: Aldridge RD, Sever DM, Eds.), 2011; pp:183-264, NH: Science Publishers, Enfield.
4. Russell LD. The classification and timing of spermatogenesis. *Histological and histopathological evaluation of the testis*. (Russell LD, Ettlin RA, SinhaHikim AP, Clegg ED, eds.), 1990; Pp: 41–58, Cache River Press, Florida.
5. Gist DH, Turner TW, Congdon JD. Chemical and thermal effects on the viability and motility of spermatozoa from the turtle epididymis. *J Reprod Fertil*. 2000; 119:271–77.

6. Gribbins KM, Gist DH. Cytological evaluation of spermatogenesis within the germinal epithelium of the male European wall lizard, *Podarcis muralis*. *J Morphol*. 2003; 258:296–306. doi: 10.1002/jmor.10143
7. Gribbins KM, Elsey RM, Gist DH. Cytological evaluation of the germ cell development strategy within the testis of the American alligator, *Alligator mississippiensis*. *Acta Zoologica*. 2006; 87:59–69. doi: 10.1111/j.1463-6395.2006.00220.x
8. Zhang L, Han XK, Li MY, Bao HJ, Chen QS. Spermiogenesis in soft-shelled turtle, *Pelodiscus sinensis*. *Anat Rec (Hoboken)*. 2007; 290:1213–22. doi: 10.1002/ar.20587
9. Griswold MD. The central role of Sertoli cells in spermatogenesis. *Semin Cell Dev Biol*. 1998; 9:411–16. doi: 10.1006/scdb.1998.0203
10. Hai Y, Hou J, Liu Y, Liu Y, Yang H, Li Z, He Z. The roles and regulation of Sertoli cells in fate determinations of spermatogonial stem cells and spermatogenesis. *Semin Cell Dev Biol*. 2014; 29:66–75. doi: 10.1016/j.semcd.2014.04.007
11. Ueno H, Mori H. Morphometrical analysis of Sertoli cell ultrastructure during the seminiferous epithelial cycle in rats. *Biol Reprod*. 1990; 43:769–76. doi: 10.1095/biolreprod43.5.769
12. Wang H, Wang H, Xiong W, Chen Y, Ma Q, Ma J, Ge Y, Han D. Evaluation on the phagocytosis of apoptotic spermatogenic cells by Sertoli cells in vitro through detecting lipid droplet formation by Oil Red O staining. *Reproduction*. 2006; 132:485–92. doi: 10.1530/rep.1.01213
13. Singh R, Cuervo AM. Lipophagy: connecting autophagy and lipid metabolism. *Int J Cell Biol*. 2012; 2012:282041. doi: 10.1155/2012/282041
14. Mizushima N, Yoshimori T, Ohsumi Y. The role of Atg proteins in autophagosome formation. *Annu Rev Cell Dev Biol*. 2011; 27:107–32. doi: 10.1146/annurev-cellbio-092910-154005
15. Singh R, Cuervo AM. Autophagy in the cellular energetic balance. *Cell Metab*. 2011; 13:495–504. doi: 10.1016/j.cmet.2011.04.004
16. Hashemi HF, Goodman JM. The life cycle of lipid droplets. *Curr Opin Cell Biol*. 2015; 33:119–24. doi: 10.1016/j.ceb.2015.02.002
17. Kabeya Y, Mizushima N, Ueno T, Yamamoto A, Kirisako T, Noda T, Kominami E, Ohsumi Y, Yoshimori T. LC3, a mammalian homologue of yeast Apg8p, is localized in autophagosome membranes after processing. *EMBO J*. 2000; 19:5720–28. doi: 10.1093/emboj/19.21.5720

18. Mizushima N, Komatsu M. Autophagy: renovation of cells and tissues. *Cell*. 2011; 147:728–41. doi: 10.1016/j.cell.2011.10.026
19. Ma Y, Yang H-Z, Xu L-M, Huang Y-R, Dai H-L, Kang X-N. Testosterone regulates the autophagic clearance of androgen binding protein in rat Sertoli cells. *Sci Rep*. 2015; 5:8894. doi: 10.1038/srep08894
20. Yefimova MG, Messaddeq N, Harnois T, Meunier A-C, Clarhaut J, Noblanc A, Weickert J-L, Cantereau A, Philippe M, Bourmeyster N, Benzakour O. A chimerical phagocytosis model reveals the recruitment by Sertoli cells of autophagy for the degradation of ingested illegitimate substrates. *Autophagy*. 2013; 9:653–66. doi: 10.4161/auto.23839
21. Chen Y, Zhou Y, Wang X, Qian W, Han X. Microcystin-LR induces autophagy and apoptosis in rat Sertoli cells in vitro. *Toxicol*. 2013; 76:84–93. doi: 10.1016/j.toxicol.2013.09.005
22. Liu C, Wang H, Shang Y, Liu W, Song Z, Zhao H, Wang L, Jia P, Gao F, Xu Z, Yang L, Gao F, Li W. Autophagy is required for ectoplasmic specialization assembly in sertoli cells. *Autophagy*. 2016; 12:814–32. doi: 10.1080/15548627.2016.1159377
23. Gribbins KM, Gist DH, Congdon JD. Cytological evaluation of spermatogenesis and organization of the germinal epithelium in the male slider turtle, *Trachemys scripta*. *J Morphol*. 2003; 255:337–46. doi: 10.1002/jmor.10069
24. Zhang L, Han X-K, Qi Y-Y, Liu Y, Chen Q-S. Seasonal effects on apoptosis and proliferation of germ cells in the testes of the Chinese soft-shelled turtle, *Pelodiscus sinensis*. *Theriogenology*. 2008; 69:1148–58. doi: 10.1016/j.theriogenology.2008.01.028
25. Meylan PA, Schuler R, Moler P, Wood R. Spermatogenic cycle of the Florida softshell turtle, *Apalone ferox*. *Copeia*. 2002; 2002:779–86. doi: 10.1643/0045-8511(2002)002[0779:SCOTFS]2.0.CO;2
26. Guillette LJ Jr, Woodward AR, Crain DA, Masson GR, Palmer BD, Cox MC, You-Xiang Q, Orlando EF. The reproductive cycle of the female American alligator (*Alligator mississippiensis*). *Gen Comp Endocrinol*. 1997; 108:87–101. doi: 10.1006/gcen.1997.6953
27. Kwiat GA, Gist DH. Annual reproductive cycle of an introduced population of European wall lizards (*Podarcis muralis*) in Ohio. *J Herpetol*. 1987; 21:205–09. doi: 10.2307/1564484
28. Hess RA. Quantitative and qualitative characteristics of the stages and transitions in the cycle of the rat seminiferous epithelium: light microscopic observations of perfusion-fixed and plastic-embedded testes. *Biol Reprod*. 1990; 43:525–42. doi: 10.1095/biolreprod43.3.525
29. Kumar M. Spermatogenesis in the house sparrow, *Passar domesticus*: histological observations. *Pavo*. 1995; 33:1–4.
30. Ahmed N, Yufei H, Yang P, Muhammad Yasir W, Zhang Q, Liu T, Hong C, Lisi H, Xiaoya C, Chen Q. Cytological study on Sertoli cells and their interactions with germ cells during annual reproductive cycle in turtle. *Ecol Evol*. 2016; 6:4050–64. doi: 10.1002/ece3.2193
31. Kerr JB, de Kretser DM. Proceedings: the role of the Sertoli cell in phagocytosis of the residual bodies of spermatids. *J Reprod Fertil*. 1974; 36:439–40. doi: 10.1530/jrf.0.0360439
32. Lofts B, Tsui H. Histological and histochemical changes in the gonads and epididymides of the male Soft-shelled turtle, *Trionyx sinensis*. *J Zool*. 1977; 181:57–68. doi: 10.1111/j.1469-7998.1977.tb04570.x
33. Shivanandappa T, Devaraj Sarkar HB. Seasonal lipid cycle and steroidogenic activity in the testis of the tropical skink, *Mabuya carinata* (Schneider): a histochemical study. *Gen Comp Endocrinol*. 1979; 38:491–95. doi: 10.1016/0016-6480(79)90158-8
34. Dupont N, Chauhan S, Arko-Mensah J, Castillo EF, Masedunskas A, Weigert R, Robenek H, Proikas-Cezanne T, Deretic V. Neutral lipid stores and lipase PNPLA5 contribute to autophagosome biogenesis. *Curr Biol*. 2014; 24:609–20. doi: 10.1016/j.cub.2014.02.008
35. Xie Z, Klionsky DJ. Autophagosome formation: core machinery and adaptations. *Nat Cell Biol*. 2007; 9:1102–09. doi: 10.1038/ncb1007-1102
36. Suzuki K, Ohsumi Y. Molecular machinery of autophagosome formation in yeast, *Saccharomyces cerevisiae*. *FEBS Lett*. 2007; 581:2156–61. doi: 10.1016/j.febslet.2007.01.096
37. Shpilka T, Welter E, Borovsky N, Amar N, Mari M, Reggiori F, Elazar Z. Lipid droplets and their component triglycerides and steryl esters regulate autophagosome biogenesis. *EMBO J*. 2015; 34:2117–31. doi: 10.15252/embj.201490315
38. Dall'Armi C, Devereaux KA, Di Paolo G. The role of lipids in the control of autophagy. *Curr Biol*. 2013; 23:R33–45. doi: 10.1016/j.cub.2012.10.041
39. Dong H, Czaja MJ. Regulation of lipid droplets by autophagy. *Trends Endocrinol Metab*. 2011; 22:234–40. doi: 10.1016/j.tem.2011.02.003
40. Rambold AS, Cohen S, Lippincott-Schwartz J. Fatty acid trafficking in starved cells: regulation by lipid droplet lipolysis, autophagy, and mitochondrial fusion

dynamics. *Dev Cell*. 2015; 32:678–92. doi: 10.1016/j.devcel.2015.01.029

41. Kuma A, Matsui M, Mizushima N. LC3, an autophagosome marker, can be incorporated into protein aggregates independent of autophagy: caution in the interpretation of LC3 localization. *Autophagy*. 2007; 3:323–28. doi: 10.4161/auto.4012
42. Obert LA, Sobocinski GP, Bobrowski WF, Metz AL, Rolsma MD, Altrogge DM, Dunstan RW. An immunohistochemical approach to differentiate hepatic lipidosis from hepatic phospholipidosis in rats. *Toxicol Pathol*. 2007; 35:728–34. doi: 10.1080/01926230701481956
43. Eid N, Ito Y, Maemura K, Otsuki Y. Elevated autophagic sequestration of mitochondria and lipid droplets in steatotic hepatocytes of chronic ethanol-treated rats: an immunohistochemical and electron microscopic study. *J Mol Histol*. 2013; 44:311–26. doi: 10.1007/s10735-013-9483-x
44. Liu T, Chu X, Huang Y, Yang P, Li Q, Hu L, Chen H, Chen Q. Androgen-related sperm storage in oviduct of Chinese Soft-Shelled Turtle in vivo during annual cycle. *Sci Rep*. 2016; 6:20456. doi: 10.1038/srep20456